*engineering proceedings*

MDPI

*1potwpot444440=)potw.*

# LWIR interband cascade photodetectors with InAs/InAsSb II type superlattice absorber

**Krzysztof Murawski[1], Kinga Majkowycz[1], Tetiana Manyk[1], Małgorzata Kopytko[1], Krystian Michalczewski[2], Jarosław Jureńczyk[2], Łukasz Kubisz[2], Bartosz Seredyński[1], Piotr Martyniuk[1]**

[1] Applied Physics Institute, Military University of Technology, 2 Kaliskiego St., 00-908 Warsaw, Poland; krzysztof.murawski01@wat.edu.pl; kinga.majkowycz@wat.edu.pl; tetjana.manyk@wat.edu.pl; malgozata.kopytko@wat.edu.pl; Bartosz.seredynski@wat.edu.pl; potr.martyniuk@wat.edu.pl;

[2] VIGO PHOTONICS S.A. 129/133 Poznańska St. 05-850 Ożarów Mazowiecki, Poland, kmichalczewski@vigo.com.pl, lkubiszyn@vigo.com.pl, jjurenczyk@vigo.com.pl

* Correspondence: krzysztof.murawski01@wat.edu.pl;Tel.: (+48 261839374)

† Presented at Advanced Infrared Technology & Applications – AITA 2025, Kobe- Japan, 15–19 September , 2025.

**Abstract:** The properties of long-wave infrared (LWIR) interband cascade photodetectors (ICIPs) with type II superlattices (T2SLs) and gallium-free (Ga-free) InAs/InAsSb absorbers were determined using photoluminescence (PL) and spectral response (SR) measurements. The heterostructures were grown by molecular beam epitaxy (MBE) on a GaAs substrate. Three structures with different numbers of stages were compared. The structures were optimized for 10.7 μm at 300 K. Moreover, theoretical calculations were performed using APSYS to compare with the experimental results. The PL results provided information on transitions from minibands and intragap states in the studied structures. SR measurements helped isolate transitions involving minibands, which facilitated the analysis of visible transitions in the PL spectra, where point defect (NPD) transitions were also observed.

**Keywords:** cascade photodetectors, InAs/InAsSb, T2SLs, photoluminescence

## 1. Introduction

New challenges for detection devices drive the continuous improvement of technologies based on semiconductor materials. The long-wave infrared region is particularly important in this context. Devices based on III–V group materials especially type-II InAs/GaSb superlattices and 'gallium-free' InAs/InAsSb (T2SL)—are increasingly used in this wavelength range. However, many challenges remain, particularly due to the larger effective masses of hole conduction in the growth direction. This effect, in turn, leads to lower vertical hole mobility and shorter diffusion lengths [1-4]. These factors significantly impact the detection parameters of the final devices.

The use of a T2SL Interband Cascade Photodetector (ICIP) helps eliminate some of these issues[5-7]. The main advantage of this concept is the reduction of overall noise, which results in a nominal increase in detectivity. Furthermore, the dark current in the ICIP is ultimately limited by generation currents from Shockley–Read–Hall (SRH) and Auger processes.

In this work, Ga-free InAs/InAsSb T2SL absorber-based ICIP devices with different numbers of stages were compared. The analysis was performed using PL and SR measurements. The results were compared with APSYS simulations and data from the literature.

**Citation:** To be added by editorial staff during production.

Academic Editor: Firstname Lastname

Published: date

## 2. Detector structure

The ICIP T2SL InAs/InAsSb structures were grown using a RIBER Compact 21-DZ solid-source MBE system on 2″ GaAs (001) substrates. A 250 nm-thick GaAs smoothing layer was first deposited directly on the substrate. This was followed by a 0.59 µm GaSb buffer layer, a heavily doped $N^+$ wide-gap contact layer, and *x* stages of the active region. Each stage consisted of a graded thin InAs/InAsSb N-type layer, an InAs/InAsSb absorber, and an AlGaAsSb:Be bulk barrier (EB). The individual stages were connected in series by InAs/InAsSb $p^{++}/n^{++}$ tunnel junctions.

A thin, heavily doped $p^+$ InAs/InAsSb layer was grown on the top to serve as a hole contact. Figure 1 shows a schematic of the tested detector structures. The structures differed in the number of active stages. Details of the technological processes can be found in the following publications: [7,8].

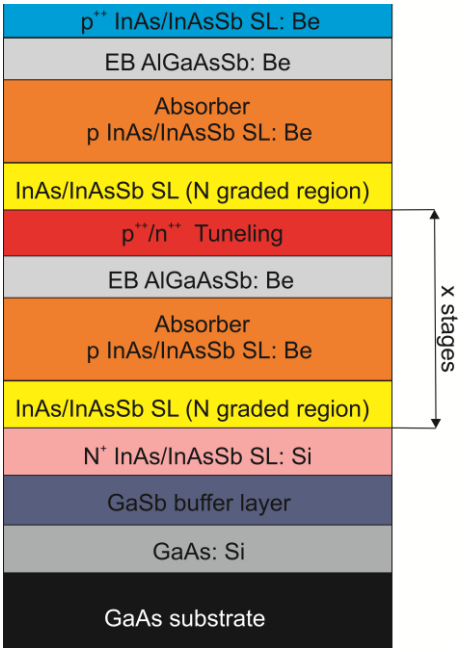


**Figure 1.** LWIR $InAs/InAs_{1-x}Sb_x$ T2SLs based ICIP.

The PL and SR spectra were collected as functions of temperature and excitation power. The measurement systems are described Ref.[9]. For measurement purposes, the structures were chemically etched down to the absorbing layer. The sample for SR measurements was mounted in a helium cryostat using a TO-8 mount. Theoretical calculations were performed using the SimuApsys platform and the 4-band k·p (8 × 8) model (Crosslight Inc.) [10].

## 3. Results and discussion

Figure 2 shows the normalized PL and SR spectra for samples with three stages (a) and five stages (b) at a temperature of 300 K. At high temperatures, the PL spectra were dominated by transitions between minibands. The black line represents the sum of all visible optical transitions.

For the three-stage structure (Fig. 2a), the D2 and D3 peaks were associated with miniband transitions. Additionally, an interband transition (D1) was observed. The corresponding energies were 85 meV, 114 meV, and 290 meV, respectively. In this case, the D2 transition was attributed to the HH1→C1 transition, which was confirmed by SR results (dashed blue line). The positions of these transitions were determined using the method described in Refs.[11]. **a**nd those occurring within the energy gap were identified using a Gaussian density of states model.

For the five-stage structure (Fig. 2b), the PL spectrum shows two visible transitions: D1 and D2, with energies of 114 meV and 205 meV, respectively. These transitions were likely associated with miniband transitions.

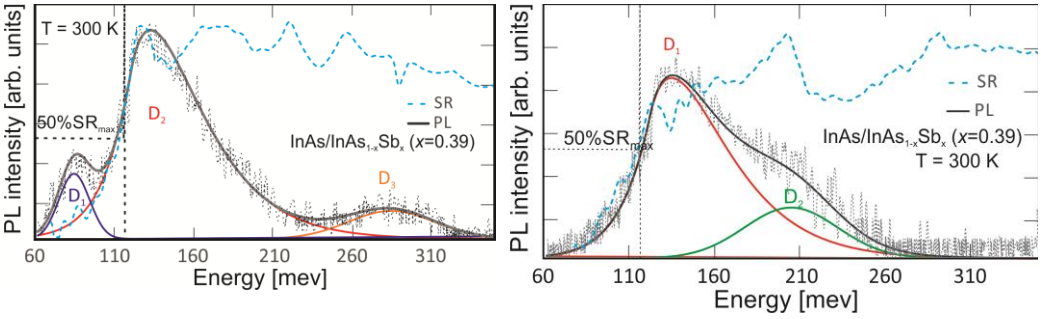


**Figure 2.** Measured PL (black solid lines), current responsivity (dashed blue lines) vs. energy for LWIR InAs/InAs$_{1-x}$Sb$_x$ T2SLs ($x_{Sb}$ = 0.39) at 300 K, (a) 3 stages, (b) 5 stages

Additionally, the experimental results were compared with APSYS simulations. The results demonstrated the influence of the number of stages on the visible transitions in the PL spectrum. Both the nature and positions of the observed transitions were confirmed by the simulations.

## 4. Conclusions

Experimental PL and SR results for LWIR ICIPs with InAs/InAsSb absorbers were presented. Measurements were performed on samples with different numbers of stages. The PL results provided information on transitions from minibands and intra-gap states in the studied structures. SR measurements helped to isolate miniband transitions , which facilitated the analysis of visible transitions in PL spectra. However, transitions with a NPD were also observed. Correlations were observed between the number of stages and the visible optical transitions in the PL spectra. Additionally, the number of stages was found to influence the position of transitions involving minibands. The experimental results were consistent with APSYS simulation data.

**Author Contributions:** Conceptualization, K.M.; methodology, K.M. and M.K.; validation, K.M., T.M. and K.M.; formal analysis, K.M. investigation, K.M. and J.J.; resources, K.M.; data curation, K.M., Ł. K., B.S, P. M.; writing—original draft preparation, K.M.; writing—review and editing, K.M. and Ł. K.; visualization, K.M.; supervision, P.M.; project administration, K.M.; funding acquisition, M.K. All authors have read and agreed to the published version of the manuscript."

**Funding:** This research was funded by National Science Centre grant: OPUS UMO-2021/43/B/ST7/01393.

**Data Availability Statement:** The data that support the funding of this study are available from the corresponding author, K.M., upon request.

**Conflicts of Interest:** The authors declare no conflict of interest.

## References

(1) Klipstein, P.; Benny, Y.; Gliksman, S.; Glozman, A.; Hojman, E.; Klin, O.; Langof, L.; Lukomsky, I.; Marderfeld, I.; Nitzani, M. Minority carrier lifetime and diffusion length in type II superlattice barrier devices. *Infrared Physics & Technology* **2019**, *96*, 155-162.

(2) Soibel, A.; Ting, D. Z.; Khoshakhlagh, A.; Bouschet, M.; Fisher, A. M.; Pepper, B. J.; Gunapala, S. D. Hole diffusion length and mobility of a long wavelength infrared InAs/InAsSb type-II superlattice nBn design. *Applied Physics Letters* **2024**, *125* (17). DOI: 10.1063/5.0236096 (acccessed 1/22/2025).

(3) Steenbergen, E. H.; Connelly, B. C.; Metcalfe, G. D.; Shen, H.; Wraback, M.; Lubyshev, D.; Qiu, Y.; Fastenau, J. M.; Liu, A. W. K.; Elhamri, S.; et al. Significantly improved minority carrier lifetime observed in a long-wavelength infrared III-V type-II superlattice comprised of InAs/InAsSb. *Applied Physics Letters* **2011**, *99* (25). DOI: 10.1063/1.3671398 (acccessed 1/21/2025).

(4) Taghipour, Z.; Lee, S.; Myers, S. A.; Steenbergen, E. H.; Morath, C. P.; Cowan, V. M.; Mathews, S.; Balakrishnan, G.; Krishna, S. Temperature-Dependent Minority-Carrier Mobility in p-Type InAs/GaSbType-II-Superlattice Photodetectors. *Physical Review Applied* **2019**, *11* (2), 024047. DOI: 10.1103/PhysRevApplied.11.024047.

(5) Martyniuk, P.; Rogalski, A.; Krishna, S. Interband quantum cascade infrared photodetectors: Current status and future trends. *Physical Review Applied* **2022**, *17* (2), 027001.

(6) Lei, L.; Li, L.; Ye, H.; Lotfi, H.; Yang, R. Q.; Johnson, M. B.; Massengale, J. A.; Mishima, T. D.; Santos, M. B. Long wavelength interband cascade infrared photodetectors operating at high temperatures. *Journal of Applied Physics* **2016**, *120* (19). DOI: 10.1063/1.4967915 (acccessed 1/22/2025).

(7) Benyahia, D.; Michalczewski, K.; Hackiewicz, K.; Kębłowski, A.; Martyniuk, P.; Rutkowski, J.; Piotrowski, J. Molecular beam epitaxy growth and characterization of interband cascade infrared detectors on GaAs substrates. *Journal of Crystal Growth* **2020**, *534*, 125512.

(8) Gawron, W.; Kubiszyn, Ł.; Michalczewski, K.; Piotrowski, J.; Martyniuk, P. Demonstration of the longwave type-II superlattice InAs/InAsSb cascade photodetector for high operating temperature. *IEEE Electron Device Letters* **2022**, *43* (9), 1487-1490.

(9) Murawski, K.; Majkowycz, K.; Kopytko, M.; Manyk, T.; Dąbrowski, K.; Seredyński, B.; Kubiszyn, Ł.; Martyniuk, P. Optical Characterization of the Interband Cascade LWIR Detectors with Type-II InAs/InAsSb Superlattice Absorber. *Nanomaterials* **2024**, *14* (17), 1393.

(10) Birner, S. Modeling of semiconductor nanostructures and semiconductor-electrolyte interfaces. **2011**.

(11) Murawski, K.; Kopytko, M.; Madejczyk, P.; Majkowycz, K.; Martyniuk, P. HgCdTe energy gap determination from photoluminescence and spectral response measurements. *Metrology and Measurement Systems* **2023**, *30* (1).